Theoret. Appl. Mech., Vol.31, No.3-4, pp. 345–360, Belgrade 2004

Particle dynamics simulations of expansion of a cylindrical cavity within an infinite brittle medium

Sreten Mastilović * **Dušan Krajčinović** †

Abstract

The present review focuses on the plane strain problem of high strain rate expansion of a cylindrical cavity within an infinite brittle material with random microstructure. The material is represented by an ensemble of "continuum particles" forming a two-dimensional geometrically and structurally disordered lattice. The proposed model includes the aleatory variability and epistemic uncertainty of the process. The dynamic particle simulations are performed at seven different cavity expansion rates. The resulting damage evolution process is non-stationary, nonlocal, and non-equilibrium. This problem, therefore, belongs to the class of phenomena for which the traditional continuum models are not well suited, and detailed experimental data are either difficult to get or not available at all. The present study explores the potential role of the particle dynamics in addressing these problems.

Key words: dynamic fracture, particle dynamics, lattice, disorder, microcracking.

*Center for Multidisciplinary Studies, University of Belgrade, Kneza Višeslava 1a, 11030 Belgrade, Serbia and Montenegro, e-mail: gmvv@eunet.yu

†Mechanical and Aerospace Engineering, Arizona State University, Tempe, Arizona 85287-6106, USA, e-mail: dusan@asu.edu

1 Introduction

The importance of deformation processes evolving at high strain rates is exceeded only by their complexity. The considered thermodynamic processes are non-stationary, non-local, and far from equilibrium. Thus, the conventional models of continuum mechanics based on the thermodynamics with internal variables are ultimately limited, despite the fact that they have yielded many useful findings and continue to be of great use, especially in industry. Currently used continuum modeling is more often than not based on the rate-type constitutive equations of traditional viscoplasticity. Computational codes for large deformation, high strain rate, transient phenomena are in literature usually referred to as hydrocodes (Meyers [18]). The unquestionable merit of these codes, especially in replicating the test data, is somewhat tarnished by their limited predictive capability. Moreover, despite of the truly enormous progress in experimental methods in the last three decades the available data leave a lot to be desired.

The objective of this study is to explore potential of particle dynamics (PD) simulations for providing a more detailed insight into the phenomena of the high strain rate loading of brittle materials with random microstructure. The PD method is well established as a useful tool for extrapolation of the experimental results into the regions that are beyond the present experimental capabilities. The ultimate goal of using these simulations is to facilitate formulation of rational analytical models from consideration of the damage evolution processes on the mesoscale. This analytical approach incorporates both variability and uncertainty in a straightforward manner. Variability, also termed randomness or aleatory variability, is the natural randomness in a process. Uncertainty, also termed epistemic uncertainty, is the uncertainty in the model; it is due to limited knowledge or data or both.

The mesoscale material texture is an example of the aleatory variability. The disorder may be topological (unequal coordination number), geometrical (unequal length of bonds) or structural (unequal strength and stiffness of bonds). The disorder is further enhanced by damage evolution, which is governed (to an extent depending on the deformation rate) by the local fluctuations of the energy barriers quenched within

the material and the local fluctuations of stress.

2 Particle lattice and particle dynamics

The approximation of a material by a particle lattice is inspired by the mesoscale morphology of a certain class of brittle materials, and successes of molecular dynamics method (for overview of molecular dynamics, see, for example, Hoover [11] and Allen and Tildesley [1]). On the other hand, the lattice used in molecular dynamics simulations is inspired by the discrete morphology of an ensemble of atoms. Thus, the PD can be considered an engineering offshoot of the molecular dynamics. Within this framework, continuum can be defined as a collection of discrete elements, known as "continuum particles" (Wiener 1983) whose location and momenta are determined by solving a system of ordinary differential equations of Hamiltonian mechanics. A number of numerical techniques are available to accomplish this task, including the most widely used the Verlet, Störmer, and Gear predictor-corrector algorithms. The choice of the solution technique is largely a matter of preference since all of these methods are stable as long as the time step is carefully selected (Hoover [11], Allen and Tildesley [1]).

In the present study the brittle material is approximated by a two-dimensional triangular lattice[1] equivalent to a three-dimensional elastic continuum under a plane strain condition (Monette and Anderson [19]). A particle may represent a grain of ceramic, a concrete aggregate or a granule of clastic rock. The average distance between two neighboring particles ($\bar{\lambda}$) is, therefore, the model resolution length ($\mathrm{l_c}$). Hence, the effect of all defects smaller than the resolution length and the residual stress along the grain boundary must be introduced through the strength distribution. An important advantage of the lattice approximation of a solid is that the statistical nature of the structural, geometrical, and topological defects on the micro and meso scales is introduced in a natural manner.

The particles (of mass m) located in lattice nodes interact through

[1] A Delaunay graph dual to Voronoi polygons representing random grains (Krajcinovic [12]). (For a detailed discussion of the Voronoi tessellation, including the digitalization of micrographs, see Espinosa and Zavattieri [7].)

the central-force links with their nearest neighbors. The properties of these bonds are approximated by a linear force-elongation relation in tension (Hookean potential for a perfectly brittle material), and a non-linear force-deformation relation in compression (Figure 1).

The force-deformation relation in compression ($\lambda_{ij} < \lambda_{0ij}$) is:

$$F_{ij}^R = \frac{k_{ij}\lambda_{0ij}}{(B-2)}\left\{\exp\left[B\left(1-\left(\frac{\lambda}{\lambda_0}\right)_{ij}\right)\right]-\left(\frac{\lambda_0}{\lambda}\right)_{ij}^2\right\} \qquad (1)$$

where λ_{0ij} and λ_{ij} are the initial and current distances separating interacting particles i and j, k_{ij} corresponding link stiffness, while the parameter B defines the slope (steepness) of the repulsive wall. The relation (1) is inspired by the Born-Meyer potential, which was originally developed to model closed-shell repulsion in ionic crystals (Born and Huang [5], Vitek [23]). This force-deformation relation captures dominant mechanical features of the quasi-brittle materials such as brittle behavior in tension, increase of shock wave velocity and decrease of compressibility with increasing pressure.

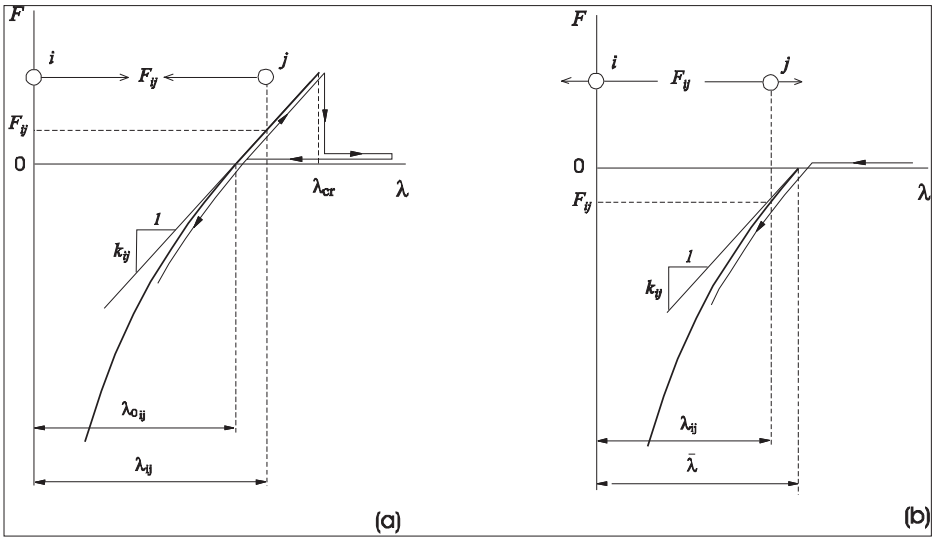

Figure 1: Nonlinear elastic–brittle relation between the link force and deformation. Interaction between particles that (a) are or were initially the nearest neighbors, (b) were not initially the nearest neighbors

The interaction of particles is limited to the nearest neighbors. The nearest-neighbors approximation is based on the primacy of the short-range order (Zallen [25]), and motivated by straightforward crack definition and tremendous computational savings (of solving O(N) rather than $O(N^p)$ problem, where N is the number of particles in the system, and $p \geqslant 2$ the interaction range parameter).

The size of grains and strength of grain boundaries in a polycrystalline ceramics are stochastic parameters. The lattice morphology is defined by the coordination number z and link length λ. The strength of a grain boundary is affected by randomly distributed residual stresses (Curtin and Scher [6]), twist and tilt angles, dislocations, second phase particles, and other imperfections.

In the pristine state all lattices used in this study are topologically ordered by selecting $z = 6$ for all bulk-particles. The lattice is geometrically disordered since the equilibrium distances between particles (initial link lengths $\equiv \lambda_0$) are sampled from the normal distribution within the range $\left[\alpha\bar{\lambda} \leqslant \lambda_0 \leqslant (2-\alpha)\,\bar{\lambda}\right]$, (Figure 2a). Model parameter $\alpha_l, (0 < \alpha_l \leqslant 1)$, defines bandwidth of the geometrical disorder of material (i.e., the distribution of grain sizes). The lattice is also structurally disordered due to the random distribution of link strengths and stiffnesses. The link stiffnesses are uniformly distributed within the range $\left[\beta\bar{k} \leqslant k \leqslant (2-\beta)\,\bar{k}\right]$, (Figure 2b), where β_l, $(0 \leqslant \beta_l \leqslant 1)$, is stiffness distribution parameter, and $\bar{k} = 8\,E_0/5\sqrt{3}$ mean link stiffness related to the modulus of elasticity of the pristine material, E_0 (Monette and Anderson [19]).

The link-rupture criterion is defined in terms of the critical link elongation. That is, the link between particles $i$and j ruptures (as its force-carrying capacity in tension is permanently lost) when the link elongation reaches the critical value $\varepsilon_{ij} = \Delta\lambda_{ij} \;/\; \lambda_{0ij} = \varepsilon_{cr} = const.$ The critical link elongation, ε_{cr}, is the model parameter related to the uniaxial tensile strength of the material.

The selected model recognizes two different types of interaction between particles: chemical and mechanical. The chemical interaction is both tensile and compressive, and is limited to the nearest neighbors. The mechanical interaction is strictly compressive, but the number of involved particles is not limited. It can be established between particles that were either initially not connected or re-established between

particles that were previously separated by the link rupture. In the former case the mechanical link is established when the initial distance between particles shrinks below the average link length $\bar{\lambda}$ (Figure 1b). In the latter case the repulsive interaction is re-established when the distance between particles reduces to $\lambda_{ij} \leqslant \lambda_{0ij}$ (Figure 1a).[2] The formation of the mechanical (repulsive) force between the particles that were not connected by cohesive forces is essential to model the flow of the comminuted phase.

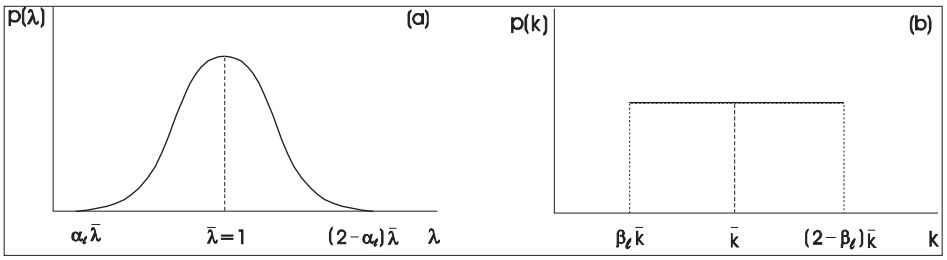

Figure 2: Probability distribution of (a) link lengths and (b) link stiffnesses

The computer simulations of the cylindrical cavity expanding in the lattice are conceptually very simple. The cavity is nucleated by removing a single particle in the middle of the lattice. After the cavity formation all particles that are located along the cavity perimeter are pushed away in radial direction at a controlled expansion rate $v_r^c = \dot{a}$ (where a is the cavity radius, dot denotes differentiation with respect to time, while subscript r and superscript c indicate the radial direction and the cavity perimeter, respectively). In this study the cavity expansion rate, v_r^c, was held constant during the simulation. The simulation is terminated when the longitudinal elastic wave (P wave) reaches the plate boundary to eliminate the boundary effects (i.e., to simulate the cavity expansion within an infinite medium). The lattice is divided into five annular regions of equal width over which a particular field parameter or property is averaged. As the cavity expands the absolute widths of the annular regions necessarily shrink, but the relative widths are kept unchanged.

[2]Preventing the transmission of tensile force by mechanical contact (Figure 1b) is tantamount to assuming that a ruptured bond cannot heal.

The parameters recorded through the entire process within each annular zone are: the position and velocity of each particle, number of ruptured links, and force in each link. Calculation of the deformation and kinetic energy in each annular region, knowing the position and velocity of each particle, is straightforward. The density of isotropic damage is defined by the fraction of broken bonds $D = n/N$, where n and N are the number of broken bonds and the total number of bonds, respectively. The statistical mechanics expressions for the components of the stress and effective stiffness tensors are adopted from the conventional molecular dynamics (Weiner 1983, Vitek 1996).

3 Results

The simulations are performed for seven different cavity-expansion velocities $v_r^c = \theta \cdot C_L$, where $\theta = 0.135, 0.08, 0.04, 0.022, 0.0135, 0.007, 0.00135$, while C_L is the velocity of longitudinal elastic wave propagation. The lattice is formed by approximately 12000 particles of the following geometric and structural parameters: the average (mean) link stiffness $\bar{k} = 50$, average equilibrium distance between particles $\bar{\lambda} = 1$, geometrical disorder parameter $\alpha_l = 0.001$, stiffness distribution parameter $\beta_l = 0.6$, repulsive wall parameter $B = 5$, and critical strain of the link $\varepsilon_{cr} = 0.1\%$.[3] (For discussion of the non-dimensional parameters see Allen and Tildesley [1].)

The radial tractions at the cavity perimeter, components of effective stiffness and stress tensors, damage density, kinetic and deformation energy, and the energy released by link rupture are computed in each simulation step. The evolution curves are available in Mastilovic and Krajcinovic [17].

The experimental observations (Shockey et al. [21], Strassburger

[3]It seems appropriate to emphasize that the mean link stiffness, $\bar{k} = 8\,E_0/5\,\sqrt{3}$, and critical strain of the link, ε_{cr}, are directly related to the measurable macroscopic properties of the material, namely modulus of elasticity and the failure strain, respectively. The repulsive wall parameter B could be inferred from the ballistic equation of state. Its identification, therefore, requires a combination of the experimental and simulation data. The disorder parameters α_l and β_l have to be, at present, arbitrarily selected, due to their epistemic uncertainty (i.e., almost total absence of detailed micrographic data).

and Senf [22]) and PD simulations presented in this review (Figure 3) indicate that the damage evolution pattern is strongly dependent on the cavity expansion velocity (rate). When the cavity expansion rate (and the corresponding externally imparted energy) is modest, the microcracks tend to localize into few macrocracks propagating in a radial direction away from the cavity (Figures 3c and 3d).[4] At cavity expansion rates in excess of a critical magnitude, v_{rT}^c, the material near the hole is shattered by the overwhelming imparted energy (Figure 3a).

An approximate expression for the damage-mode transition velocity, derived by Mastilovic and Krajcinovic [15] based on the PD simulation results, is:

$$v_{rT}^c = \frac{1+\upsilon_0}{1-\upsilon_0} \cdot \sqrt{\frac{3\ (1-2\,\upsilon_0)}{(1+\upsilon_0)\cdot(3-2\upsilon_0)} \cdot \sigma_f}\ \cdot\ C_L \tag{2}$$

where υ_0 and σ_f are the Poisson's ratio and the uniaxial tensile strength of the material in the pristine (damage-less) state, respectively.

It is important to recognize diminishing of the importance of the local fluctuations of the energy barriers (quenched within the material) and the local fluctuations of stress on the damage evolution with increase of the energy carried by the stress waves (i.e., with increase of the loading rate). To put it plainly, the high-intensity stress waves "have no use" for the subtlety of the material morphology. This discussion echoes Anderson's [2] conclusions that: (1) localization is impossible in the absence of disorder and (2) the localization range depends on the frequency and energy of electron waves.

The scope of the following discussion is limited largely to the high-velocity expansion (Figure 3a). According to the simulation data, available in Mastilovic and Krajcinovic [17], the damage pattern in Figure 3a is distinguished by three distinct regions. Material within the transformed (Mescall) region adjacent to the expanding cavity is commin-

[4]The formation of patterns and shapes associated with non-equilibrium growth and relation between the macroscopic driving force and microscopic dynamics has been and still is a fascinating field of research. The damage patterns obtained from the PD simulations resemble morphologies of the Helle-Shaw cells studied extensively in the last two decades (for example, see Ben-Jacob and Garik [4] or, for crack-growth application, Hermann and Kertesz [9]).

uted (crushed, pulverized) ($D \approx 1, \dot{D} \approx 0$). Material within the process region is damaged ($0 < D < 1, \dot{D} > 0$) but still able to transmit tensile stresses. The annular elastic region, furthest from the cavity, is in the pristine state ($D = 0, \dot{D} = 0$).

The estimation of the radial traction along the cavity perimeter σ_r^c is one of the most interesting and important aspects of the simulation. The dependence of the radial traction on the strain rate reflects the quantitative difference between damage evolution modes shown in Figure 3. At the high rate of the cavity expansion (Figure 3a), the evolution of the radial tractions σ_r^c is characterized by a sharp peak, followed by a steep relaxation, and stagnation (Figure 4). The peak magnitudes of the radial traction (the full circles in Figure 4) are in very good agreement with the analytical solution for the radial stress at the elastic wave front at the perimeter of an expanding cavity (Kromm [14]).

Fortuitously or not, the data in Figure 4 indicate that the average stagnation values of the radial tractions at the cavity perimeter vary within a narrow band of (0.32 – 0.36) of the corresponding peak values for all three high-expansion-rate cases. Based on this observation, the stagnation magnitude[5] of the radial traction at the cavity perimeter characterizing long-time response can be obtained in the following form:

$$\langle \sigma_r^c \rangle = \frac{1 - \upsilon_0}{1 + \upsilon_0} \cdot \frac{v_r^c}{C_L} \cdot K_0 \tag{3}$$

where K_0 is the bulk modulus of the pristine material. The traction values obtained by using Eq. (3) are shown in Figure 4 by hollow squares.

The dependence of the long-time radial traction along the cavity perimeter on the cavity-expansion velocity, illustrated in Figure 5, is essential for analytical modeling of the material response to this type of loading. The data points marked by hollow squares represent the simulation estimates for seven different cavity-expansion velocities (notice that only three highest-velocity cases are presented in Figure 4, the remaining four curves are available in Mastilovic and Krajcinovic [17]). The full circle denotes an analytical solution for static expansion of a cylindrical cavity in an infinite brittle material (Forrestal and Longcope

[5]Defined as the time average: $\langle \sigma_r^c \rangle = \lim_{t \to \infty} \frac{1}{t} \int_{t_0}^{t_0+t} \sigma_r^c(\tau)\, d\tau$ (Krajcinovic [12])

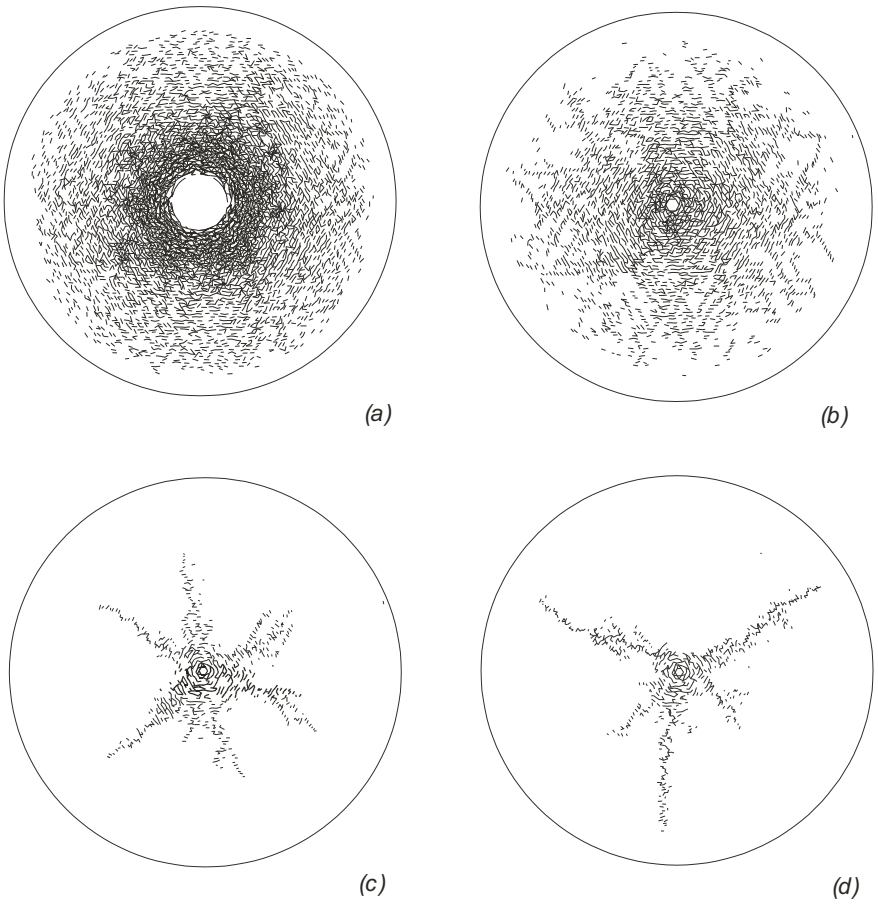

Figure 3: Dependence of the damage evolution pattern on the velocity of cavity expansion: (a) $v_r^c = 0.135\, C_L$, (b) $v_r^c = 0.0135\, C_L$, (c) $v_r^c = 0.00135\, C_L$, and (d) $v_r^c = 0.000135\, C_L$. The cracks are perpendicular to the ruptured links (indicated by short lines)

[8]). According to Figure 5, the simulation data for low-velocity cavity expansion asymptotically approaches the static solution. The solid and dashed lines represent the data approximation by a bilinear curve and a second order polynomial, respectively. Both curves are obtained by using the static solution and two data points based on Eq. (3).

Previously discussed transition from the localized to distributed damage occurs approximately within the shaded area in Figure 5. (The in-

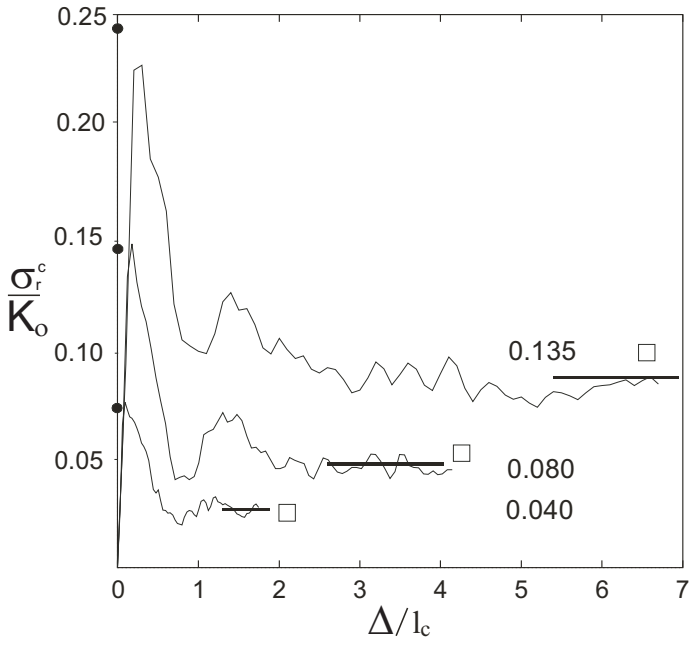

Figure 4: Radial traction along the perimeter of the expanding cavity plotted vs. change of cavity radius for the three following velocities of cavity expansion: $v_r^c = 0.040\, C_L$, $v_r^c = 0.080\, C_L$, and $v_r^c = 0.135\, C_L$. (Note: $l_c = \bar{\lambda}$ is the resolution length, and $\Delta(t) = a(t) - a_0$ is the change of cavity radius during expansion, such that $v_r^c = \dot{\Delta} = \dot{a} = const.$; thus, $\Delta/l_c \propto t$)

terception of the two straight lines defines the damage-mode transition velocity given by Eq. (2).) According to the PD simulation results, the transition region is characterized by balance between the kinetic and deformation energy ($E_k \approx U$). Notice that Nakamura et al. (as cited by Anderson [3]) used the equality of the kinetic energy and deformation energy to define a transition time between a short-time response (inertial effects are significant) and a long-time response (essentially quasi-static) of a dynamically loaded specimen.

Finally, the simulation observations and data are used in Mastilovic and Krajcinovic [17] to derive an analytical model for the high-velocity expansion of a cylindrical cavity for the axially symmetric, elastic-damaged-

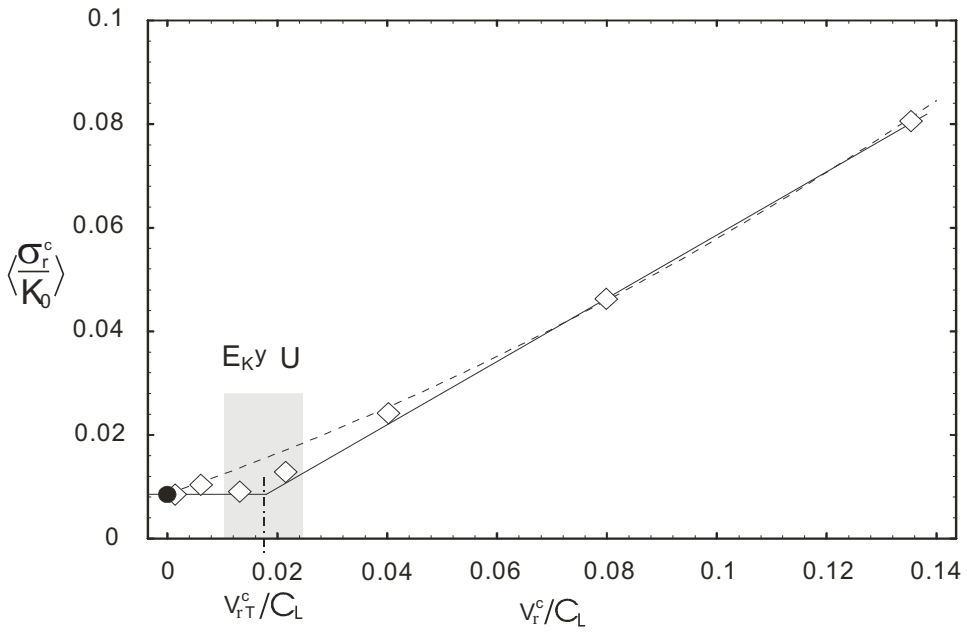

Figure 5: Radial traction along the cavity perimeter plotted vs. velocity of the cavity expansion

comminuted damage evolution pattern (Figure 3a).

4 Conclusion

This study provides insight into the process of high-velocity expansion in the brittle material and the transition from the statistically uniform damage evolution mode to the localized damage evolution mode on an example that is of significance in many fields of engineering. The obtained PD simulation results demonstrate importance of material disorder and provide an indication that PD simulations may be useful in the research of critical state. The resulting damage evolution process is non-stationary, non-local, and non-equilibrium. These problems belong to the class of phenomena for which the traditional continuum models are of limited value, and detailed experimental data are either difficult to get or not available at all. The present review suggests that PD sim-

ulations have a potential to fill these gaps to a certain extent. There is no doubt that, to paraphrase Hoover [10], the main contributions of the particle simulations remain to be understanding, semiquantitative estimates, and the capability to interpolate and extrapolate experimental data into regions that are hard to reach in the laboratory. Nonetheless, possibility of an extension of this traditional role of the molecular and particle dynamics to model elastic, plastic, and brittle behavior in a solid has been recognized in the last decade (as an example, see Scagnetti et al. [20]). A prominent aspect of the PD method is the ability to introduce the material texture (with all of its statistical subtlety) in a natural manner. All material parameters of the particle lattice can be unambiguously identified and determined from the experimental data. The virtually unlimited control over the "computational experiment" offers insights in qualitative and quantitative aspects of damage evolution in the considered class of materials subjected to dynamic loading, and potential to infer data necessary for rational analytical modeling. The present study is a successful realization of that potential.

References

[1] M.P. Allen and D.J. Tildesley (1987) Computer Simulation of Liquids, Oxford University Press Inc., New York

[2] P.W. Anderson (1958) Absence of Diffusion in Certain Random Lattices, Phys. Rev., 109, 1492-1505

[3] T.L. Anderson (1991) Fracture Mechanics, CRC Press, Boston

[4] E. Ben-Jacob and P. Garik (1990) The formation of patterns in non-equilibrium growth, Nature, 343, 523

[5] M. Born and K. Huang (1956) Dynamical Theory of Crystal Lattices, Clarendon Press, Oxford

[6] W.A. Curtin and H. Scher (1990) Brittle fracture in disordered materials: a spring network model, J. Mater. Res., 5, 535-553

[7] H.D. Espinosa and P.D. Zavattieri (2003) A grain level model for the study of failure initiation and evolution in polycrystalline brittle materials. Part I: Theory and numerical implementation, Mechanics of Materials, 35, 333-364

[8] M.J. Forrestal and D.B. Longcope (1990) Target strength of ceramic materials for high-velocity penetration, J. Appl. Phys., 67, 3669-3672

[9] H.J. Hermann and J. Kertesz (1991) Stability analysis of crack propagation, Physica A, 178, 227-235

[10] W.G. Hoover (1983) Nonequilibrium molecular dynamics, Ann. Rev. Chem., 34, 103-127

[11] W.G. Hoover (1986) Molecular Dynamics, Springer-Verlag, Berlin.

[12] D. Krajcinovic (1996) Damage Mechanics. North-Holland, Amsterdam.

[13] D. Krajcinovic and S. Mastilovic (1999) Statistical models of brittle deformation Part I: Introduction, Int. J. Plasticity, 15, 401-426

[14] A. Kromm (1948) Zur Ausbreitung von Stosswellen in Kreislochscheiben, Zeitschrift fuer Angewandte Mathematic und Mechanik, 28, 104-114

[15] S. Mastilovic and D. Krajcinovic (1999) Penetration of Rigid Projectiles Through Quasi-Brittle Materials, J. Appl. Mech., 66, 585-592

[16] S. Mastilovic and D. Krajcinovic (1999) Statistical models of brittle deformation Part II: Computer simulations, Int. J. Plasticity, 15, 427-456

[17] S. Mastilovic and D. Krajcinovic (1999) High-velocity expansion of a cavity within a brittle material, J. Mech. Phys. Solids, 47, 557-610

[18] M.A. Meyers (1994) Dynamic Behavior of Materials, John Wiley and Sons, New York

[19] L. Monette and M.P. Anderson (1994) Elastic and fracture properties of the two-dimensional triangular and square lattices, Modelling Simul. Mater. Sci. Eng, 2, 53-66

[20] P.A. Scagnetti, R.J. Nagem, G.V.H. Sandri, and T.G. Bifano (1996) Stress and Strain Analysis in Molecular Dynamics Simulation of Solids, J. Appl. Mech., 63, 450-452

[21] D.A. Shockey, A.H. Marchand, H.R. Skaggs, G.E. Cort, M.W. Burkett and R. Parker (1990) Failure phenomenology of confined ceramic targets and impacting rods, Int. J. Impact Engng., 9, 263-275

[22] E. Strassburger and H. Senf (1995) Experimental Investigation of Wave and Fracture Phenomena in Impacted Ceramics and Glasses, U. S. Army Research Lab., Aberdeen

[23] V. Vitek (1996) Pair potentials in atomistic computer simulations, In: Interatomic potentials for atomistic simulations, MRS Bulletin, 21, 20-23

[24] J.H. Wiener (1983) Statistical Mechanics of Elasticity, J. Willey and Sons, New York

[25] R. Zallen (1983) The Physics of Amorphous Solids, J. Willey and Sons, New York

Submitted on November 2004.

Širenje cilindričnog otvora u krtom materijalu: evolucija oštecenja

UDK 539.42

U radu se razmatra problem širenja cilindričnog otvora u beskonačnom krtom materijalu sa stohastičkom mikrostrukturom, pri velikim brzinama deformisanja, i u uslovima ravanskog stanja deformacija. Materijal je predstavljen skupinom "čestica kontinuuma" koje sacinjavaju dvodimenzionalnu, geometrijski i strukturno stohastičku (disordered)

mrežu, i koje su u medjusobnoj interakciji preko nelinearnih centralnih sila. Izloženi model uzima u obzir neizvesnu (aleatornu) promenljivost i epictemičku neodredjenost razmatranog procesa. Simulacije širenja otvora u opisanoj mrezi su izvršene za sedam razlicitih brzina deformisanja, korišćenjem metode dinamike čestica. U svakom vremenskom koraku beleže se: radijalni napon na obodu otvora, komponente tenzora napona i efektivne čvrstoce, gustina izotropnog oštećenja, kinetička i potencijalna energija, i energija oslobodjena kidanjem medjucestičnih veza. Rezultujuci process evolucije oštecenja je nestacionaran, nelokalan, i neravnotezan. Dotična fizicka pojava, dakle, pripada kategoriji za koju tradicionalni modeli mehanike kontinuuma nisu najpodesniji, a detaljnih eksperimentalnih podataka je ili malo ili ih uopšte nema. Ovaj rad je posvećen istraživanju mogućnosti mehanike čestica u rešavanju ovakvih problema.